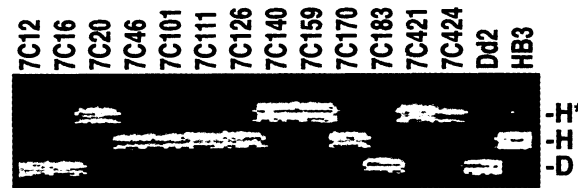


**Fig. 5.** Evidence of a spontaneous microsatellite length change in the HB3 population detected by marker TA101. The upper band (H\*) in the HB3 lane indicates the presence of a noncanonical allele in the parental population. Signals from the 7C20, 7C140, 7C159, 7C421, and 7C424 parasites show that this mutant allele was inherited exclusive of the canonical HB3 or Dd2 alleles (H, D).



**References and Notes**

1. D. Butler, *Nature* **388**, 701 (1997); E. Bond and M. J. F. Austin, *Science* **275**, 1051 (1997); T. E. Wellems, X. Su, M. Ferdig, D. A. Fidock, *Curr. Opin. Microbiol.* **2**, 415 (1999).
2. T. E. Wellems *et al.*, *Nature* **345**, 253 (1990); X. Su, L. A. Kirkman, H. Fujioka, T. E. Wellems, *Cell* **91**, 593 (1997).
3. P. Wang, M. Read, P. F. Sims, J. E. Hyde, *Mol. Microbiol.* **23**, 979 (1997).
4. A. B. Vaidya *et al.*, *Mol. Biochem. Parasitol.* **69**, 65 (1995); F. Guinet *et al.*, *J. Cell Biol.* **135**, 269 (1996).
5. K. P. Day *et al.*, *Proc. Natl. Acad. Sci. U.S.A.* **90**, 8292 (1993).
6. T. E. Wellems *et al.*, *Cell* **49**, 633 (1987).
7. R. E. L. Paul *et al.*, *Science* **269**, 1709 (1995).
8. Chromosomal DNAs were purified by pulsed-field gradient electrophoresis, cloned, and screened for simple sequence repeats by hybridization with <sup>32</sup>P-labeled (TAA)<sub>10</sub> and (T)<sub>19</sub> oligonucleotides [X. Su and T. E. Wellems, *Genomics* **33**, 430 (1996)]. Simple sequence repeats were also obtained from GenBank deposits and from the *P. falciparum* genome project, including data from recently reported sequences of chromosomes 2 and 3 [M. J. Gardner *et al.*, *Science* **282**, 1126 (1998); S. Bowman *et al.*, *Nature* **400**, 532 (1999); [www.tigr.org/tdb/mdb/pfdb/pfdb.html](http://www.tigr.org/tdb/mdb/pfdb/pfdb.html); [www.sanger.ac.uk/Projects/P\\_falciparum/](http://www.sanger.ac.uk/Projects/P_falciparum/); [www.stanford.edu/group/malaria/index.html](http://sequence-www.stanford.edu/group/malaria/index.html)]. Fluorescent detection of microsatellites was according to X. Su, D. J. Carucci, and T. E. Wellems [*Exp. Parasitol.* **89**, 262 (1998)].
9. A. Walker-Jonah *et al.*, *Mol. Biochem. Parasitol.* **51**, 313 (1992). The 35 independent progeny were isolated from the set of HB3 × Dd2 clones described by L. A. Kirkman, X. Su, and T. E. Wellems [*Exp. Parasitol.* **83**, 147 (1996)].
10. Assignments and relative order of the markers were determined by the Mapmaker program [S. E. Lincoln and E. S. Lander, *Genomics* **14**, 604 (1992); E. S. Lander *et al.*, *Genomics* **1**, 174 (1987)]. Physical assignments of 154 markers were also established with chromosome DNAs separated by pulsed-field gradient electrophoresis.
11. The full segregation data set, marker data, and mapping information are available at [www.ncbi.nlm.nih.gov/Malaria/index.html](http://www.ncbi.nlm.nih.gov/Malaria/index.html).
12. S. Karlin and U. Liberman, *Adv. Appl. Probab.* **11**, 479 (1979); U. Liberman, *J. Math. Biol.* **21**, 1 (1984). Poisson parameters were fitted to individual chromosomes as well as genome-wide crossover count distributions. Results were found to be consistent with a single count-location process, and generalized interference functions were not necessary to model the data.
13. Significant spikes of crossover activity were observed in chromosomes 12 and 9, whereas the elevation of counts seen near the RNA polymerase III gene in chromosome 13 (Fig. 3) is of marginal statistical significance ( $P = 0.06$ ). A table comparing recombination frequencies in eukaryotic organisms is available at the National Center for Biotechnology Information web site (11).
14. The theoretical line was calculated from the distributions of the distances between pairs of random points occurring uniformly within a bounded interval. Fourteen individual computations were performed on the basis of the numbers of intermarker spaces in the 14 linkage groups. The model and its expected variance were confirmed by simulations. For the purpose of calculating map parameters, all single-marker

events ( $n = 1$ ; Fig. 4) were classified as gene conversion candidates and were excluded from counts of crossovers. All other events ( $n \geq 2$ ; Fig. 4) were classified as pairs of crossovers. Assignment errors in

this classification scheme would have produced negligible consequence on the overall analysis, as they are few and tend to cancel out.

15. P. J. Hastings, *Mutat. Res.* **284**, 97 (1992).
16. The eight markers with noncanonical alleles in multiple progeny are C3M29, TA101, C4M41, BM83, P11\_1, CH12M29, C14M56, and C14M92; the other five markers are C4M76, C3M63, Y357M3, Y357M2.2, and TA88.
17. K. Hinterberg, D. Mattei, T. E. Wellems, A. Scherf, *EMBO J.* **13**, 4174 (1994).
18. We thank T. Tatusov for graphical display software; D. Severson and A. A. Schäffer for discussions on linkage analysis; and K. Pruitt, J. Ostell, and D. Lipman for advice and support. Y. Huang gratefully acknowledges sabbatical support from the China Scholarship Council.

12 July 1999; accepted 29 September 1999

## Sexual Transmission and Propagation of SIV and HIV in Resting and Activated CD4<sup>+</sup> T Cells

Z.-Q. Zhang,<sup>1</sup> T. Schuler,<sup>1</sup> M. Zupancic,<sup>1</sup> S. Wietgreffe,<sup>1</sup>  
 K. A. Staskus,<sup>1</sup> K. A. Reimann,<sup>2</sup> T. A. Reinhart,<sup>3</sup> M. Rogan,<sup>1</sup>  
 W. Cavert,<sup>1</sup> C. J. Miller,<sup>4</sup> R. S. Veazey,<sup>2</sup> D. Notermans,<sup>5</sup> S. Little,<sup>6</sup>  
 S. A. Danner,<sup>5</sup> D. D. Richman,<sup>6,10</sup> D. Havlir,<sup>6</sup> J. Wong,<sup>6,10</sup>  
 H. L. Jordan,<sup>2</sup> T. W. Schacker,<sup>7</sup> P. Racz,<sup>8</sup> K. Tenner-Racz,<sup>8</sup>  
 N. L. Letvin,<sup>2</sup> S. Wolinsky,<sup>9</sup> A. T. Haase<sup>1\*</sup>

In sexual transmission of simian immunodeficiency virus, and early and later stages of human immunodeficiency virus–type 1 (HIV-1) infection, both viruses were found to replicate predominantly in CD4<sup>+</sup> T cells at the portal of entry and in lymphoid tissues. Infection was propagated not only in activated and proliferating T cells but also, surprisingly, in resting T cells. The infected proliferating cells correspond to the short-lived population that produces the bulk of HIV-1. Most of the HIV-1–infected resting T cells persisted after antiretroviral therapy. Latently and chronically infected cells that may be derived from this population pose challenges to eradicating infection and developing an effective vaccine.

HIV-1 is usually transmitted by heterosexual contact (1) and, in prevailing hypothetical reconstructions of the initial events in infection, is believed to first infect dendritic cells (DCs) or

macrophages (Mφs) (2–11). At a later, undefined time these cell types pass infection to CD4<sup>+</sup> T cells in postulated cell-cell interactions that activate the T cells so that they become susceptible to and can support virus replication (3, 11). We experimentally examined this reconstruction of heterosexual transmission in an animal model. We inoculated 14 rhesus monkeys (*Macaca mulatta*) intravaginally with uncloned simian immunodeficiency virus (SIV) monoclonal antibody mac251, a dual tropic strain that replicates in cultured Mφs or T cell lines (12, 13). To identify the types of cells in which SIV first replicates we euthanized animals 1, 3, 7, and 12 days after inoculation and looked in tissue sections by in situ hybridization (ISH) for cells with detectable SIV RNA (14, 15). In screening  $\geq 25$  sections of tissues from the site of inoculation and distal sites in the lymphatic and other organ systems, we first detected SIV RNA in a small number of cells 3 days after inoculation only in the endocervical

<sup>1</sup>Department of Microbiology, University of Minnesota Medical School, Minneapolis, MN 55455, USA. <sup>2</sup>Division of Viral Pathogenesis, Beth Israel Hospital, Harvard University, Boston, MA 02215, USA. <sup>3</sup>Department of Infectious Diseases and Microbiology, University of Pittsburgh, Pittsburgh, PA 15261, USA. <sup>4</sup>California Regional Primate Research Center, Davis, CA 95616, USA. <sup>5</sup>Division of Infectious Diseases, Tropical Medicine and AIDS, Academic Hospital, University of Amsterdam, Academic Medical Centre, Amsterdam, 1105 AZ, Netherlands. <sup>6</sup>Departments of Pathology and Medicine, University of California, San Diego, CA 92093, USA. <sup>7</sup>Department of Medicine, University of Minnesota Medical School, Minneapolis, MN 55455, USA. <sup>8</sup>Bernhard-Nocht Institute for Tropical Medicine, Hamburg 20359, Germany. <sup>9</sup>Division of Infectious Disease, Northwestern University Medical School, Chicago, IL 60611, USA. <sup>10</sup>San Diego VA Health Care System, San Diego, CA 92093, USA.

\*To whom correspondence should be addressed.

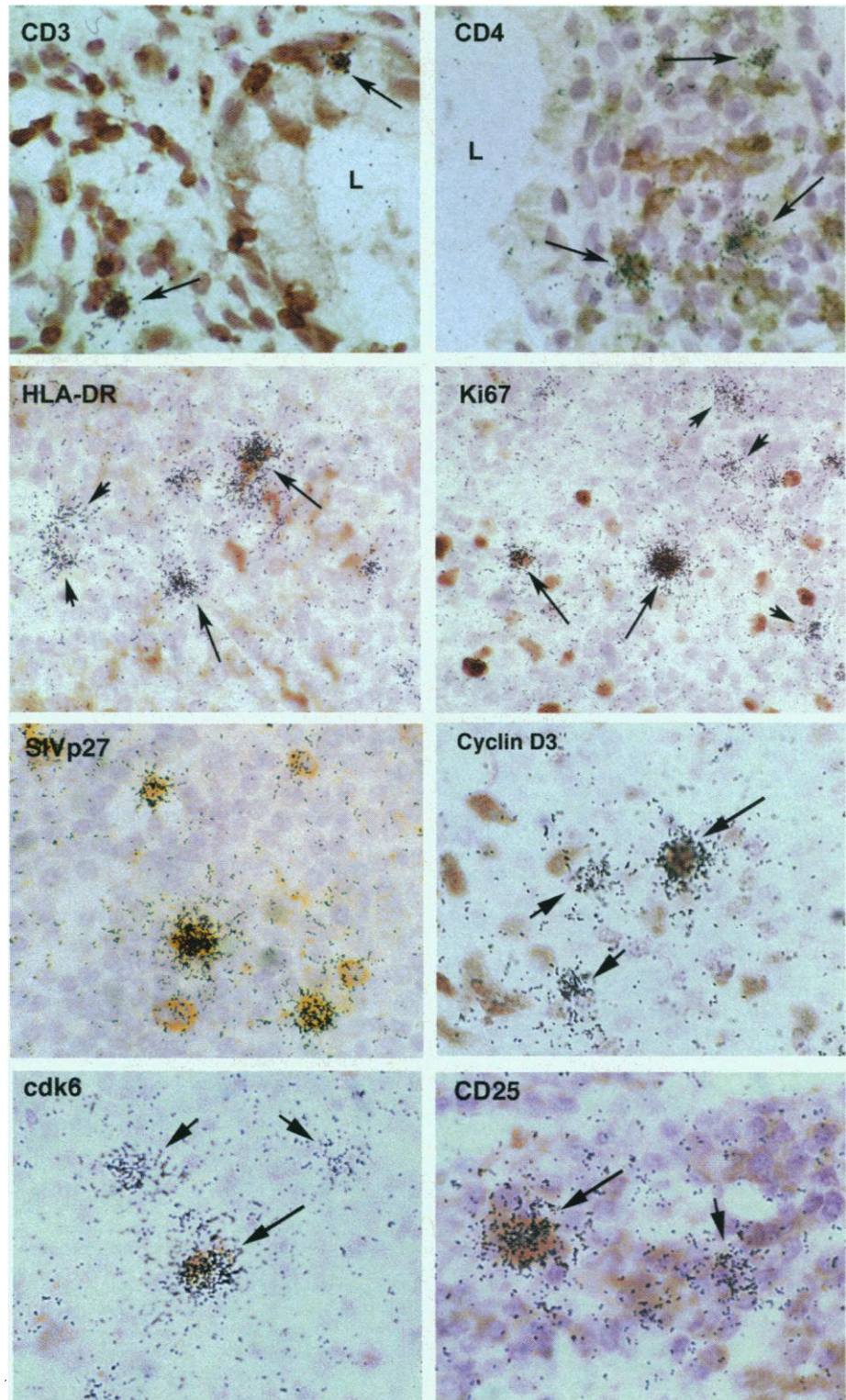
## REPORTS

region. Between days 3 and 7 there was a large increase in viral (v) RNA<sup>+</sup> cells in the endocervical region (16) followed by an additional expansion in the infected population at that site by day 12. At this time vRNA<sup>+</sup> cells were also found throughout the lymphatic tissues (LTs) and many other organs to which infection had been disseminated, with the exception of the central nervous system (Table 1).

**Fig. 1.** SIV RNA and p27 in CD3<sup>+</sup> and CD4<sup>+</sup> T cells at the portal of entry and in T cells in LNs stained or not stained by antibodies to markers of cellular activation and proliferation. Cells with SIV RNA detectable by ISH were typed IHC with antibodies that stain CD3<sup>+</sup> and CD4<sup>+</sup> T cells. Arrows in panel CD3 point to a brown-stained intraepithelial lymphocyte at the base of epithelium lining the lumen (L) of an endocervical gland and to another lymphocyte in the lamina propria with overlying collections of black silver grains indicating vRNA. In panel CD4 arrows point to CD4<sup>+</sup> vRNA<sup>+</sup> cells in lymphocytes adjacent to the lumen of a gland. In panels HLA-DR and Ki67, ISH to detect vRNA was combined with antibodies that stain activated or proliferating T cells. Longer arrows point to double-positive cells that are vRNA<sup>+</sup> and HLA-DR<sup>+</sup> or Ki67<sup>+</sup>. Short arrows point to HLA-DR<sup>-</sup> or Ki67<sup>-</sup> vRNA<sup>+</sup> cells. In panels Cyclin D3, cdk6, and CD25, longer arrows point to vRNA<sup>+</sup> cells that are also stained by antibodies to these markers of proliferation and activation. Short arrows point to vRNA<sup>+</sup> cells that lack these markers. In panel SIVp27, the major GAG core protein of SIV, there are double-positive viral p27<sup>+</sup> vRNA<sup>+</sup> cells with lower (fewer silver grains) and higher (larger numbers of silver grains) levels of vRNA.

To unequivocally identify the types of cells in which SIV was replicating, we combined ISH with immunohistochemical (IHC) staining of Mφs, DCs, and T cells (17, 18). Nearly all the vRNA<sup>+</sup> cells 3 days after inoculation were intraepithelial lymphocytes or T cells in the lamina propria of the endocervix (Fig. 1, panel CD3, and Table 2) where they may have been exposed to virus through breaks in the single

layer of epithelium lining the cervix. We characterized the host cell range for productive infection more extensively at days 7 and 12 (when there were sufficient numbers of vRNA<sup>+</sup> cells to accurately determine the frequency of the types of vRNA<sup>+</sup> cells) and documented infection in CD4<sup>+</sup> T cells (Fig. 1, panel CD4) as well as Mφs and DCs. However, close to 90% (Table 2) of the vRNA<sup>+</sup> cells at



REPORTS

the portal of entry, LTs, and other sites to which infection had been disseminated were CD4<sup>+</sup> T cells (Table 2). Because the apparent prepon-

derance of vRNA<sup>+</sup> cells in the CD4<sup>+</sup> T cell population might be the result of underestimating vRNA<sup>+</sup> Mφs or DCs with only a few

copies of vRNA, we lengthened the autoradiographic exposure to 7 days to be able to detect cells with two copies of vRNA per cell. There was no increase in the frequency of vRNA<sup>+</sup> cells and thus no evidence to support models of transmission (8-11) in which virus replicates at low levels in these other cell types, which then transmit infection to CD4<sup>+</sup> T cells. The preponderance of productive infection in CD4<sup>+</sup> T cells shortly after intravaginal transmission and similar recent observations for the intrarectal, oral, and intravenous routes collectively point to the importance of CD4<sup>+</sup> T cells in the propagation of infection after mucosal or parenteral exposure (11, 19).

**Table 1.** Tissues with viral RNA<sup>+</sup>. Cells after intravaginal inoculation of SIV. NT, not tested; -, not detected; +,  $\geq 6 \times 10^{-3}$  vRNA<sup>+</sup> cells per square millimeter of tissue (>2 copies per cell); ++,  $\geq 4.5 \times 10^{-1}$  vRNA<sup>+</sup> cells per square millimeter of tissue; +++++,  $\geq 3.5$  vRNA<sup>+</sup> cells per square millimeter of tissue.

Tissue	Day 1	Day 3	Day 7	Day 12
Vagina	-	-	-	++++
Cervix	-	+	++	++++
Draining LN*	-	-	-	++++
Distal LN†	-	-	-	++++
Other LT‡	-	-	-	++++
Bone marrow	-	-	-	++
Central nervous system§	NT	NT	-	-

\*Common, external and internal iliacs and inguinal LN. †Mesenteric, lumbar, and axillary LN. ‡Thymus, tonsil, spleen, gut-associated LT in ileum. §Frontal cortex, thalamus, basal ganglia, III, IV ventricles.

**Table 2.** Percent SIV RNA<sup>+</sup> cell types within endocervix (CVX) and axillary LNs. SIV RNA<sup>+</sup> cell types were determined by combined IHC-ISH assays of subjacent sections of endocervix in which vRNA<sup>+</sup> cells were first identified at day 3. Percentages were determined at days 7 and 12 after intravaginal inoculation of SIV by scoring  $\geq 100$  T cells stained by antibodies to CD3 and CD4<sup>+</sup> T cells stained by antibodies to CD4, Mφs stained by anti-CD68, and DCs stained by anti-S100. Because the percentages were determined independently in subjacent sections, the total amount of cell RNA<sup>+</sup> cells could be >100%. At day 3 there were sufficient numbers of vRNA<sup>+</sup> cells to accurately determine only a percentage for IHC staining with anti-CD3. The criteria for scoring vRNA<sup>+</sup> cells and the limits of sensitivity are described in (16). The longer autoradiographic exposures did not reveal larger numbers of CD68<sup>+</sup> or S100<sup>+</sup> vRNA<sup>+</sup> cells.

Days after inoculation	Tissue	CD3 <sup>+</sup>	CD4 <sup>+</sup>	CD68 <sup>+</sup>	S100 <sup>+</sup>
1	CVX	-	-	-	-
3	CVX	90	NT	NT	NT
7	CVX	79	86	11	7
12	CVX	80	89	12	6
12	LN	89	91	10	4

**Table 3.** SIV RNA levels in HLA-DR<sup>+</sup> or HLA-DR<sup>-</sup> and Ki67<sup>+</sup> or Ki67<sup>-</sup> T cells. Infected cells that were stained or not stained immunohistochemically with antibodies to the indicated markers were easily identified visually in sections of the indicated tissues 12 days after intravaginal inoculation by overlying clusters of  $\geq 10$  silver grains over background, satisfying the probability criterion of >0.995 that the cell was infected. Percentages of vRNA<sup>+</sup> cells by this criterion that were not stained by antibodies to the indicated markers were determined from 100 cells. Grain counts per cell were determined for 100 stained or unstained cells.

Tissue	Percent vRNA <sup>+</sup> T cells		Intracellular vRNA levels (grain counts per cell)			
	HLA-DR <sup>-</sup>	Ki67 <sup>-</sup>	HLA-DR <sup>+</sup>	HLA-DR <sup>-</sup>	Ki67 <sup>+</sup>	Ki67 <sup>-</sup>
CVX	67	87	330 ± 210	85 ± 61	436 ± 262	98 ± 68
LN	62	83	376 ± 254	55 ± 34	394 ± 258	57 ± 43

**Table 4.** Expansion of two infected populations of T cells after sexual mucosal transmission of SIV. Cells that met criteria for infection defined in Table 1 that were stained or not stained immunohistochemically by antibodies for the indicated markers were first detectable 3 days after intravaginal inoculation after extensive search of 20 sections of endocervix with an area of 1660 mm<sup>2</sup>. For comparison, infected cell counts at later times were normalized to this area. Semilogarithmic plots of the frequency of vRNA<sup>+</sup> cells that are HLA-DR<sup>+</sup> or HLA-DR<sup>-</sup> and Ki67<sup>+</sup> or Ki67<sup>-</sup> versus days of infection are linear; thus, both populations are expanding exponentially.

Markers		Endocervix			LN
		Day 3	Day 7	Day 12	Day 12
HLA-DR	+	14	165	1996	4,623
	-	13	729	4052	14,102
Ki67	+	22	62	990	2,825
	-	26	743	6858	18,675

We expected the vRNA<sup>+</sup> T cells to be activated and in cycle because in vitro T cell activation and lentiviral replication are generally thought to be inseparable (20). We set out to confirm that virus replication in vivo is also confined to activated and proliferating T cells by combining ISH to detect SIV RNA with IHC staining with antibodies to markers of T cell activation (HLA-DR) and proliferation (Ki67). As expected, we detected SIV RNA in cells that were activated and proliferating but, surprisingly, found also that many SIV RNA<sup>+</sup> cells were HLA-DR<sup>-</sup> and Ki67<sup>-</sup>. Although both populations of SIV RNA<sup>+</sup> HLA-DR<sup>+</sup> and Ki67<sup>+</sup> and HLA-DR<sup>-</sup> and Ki67<sup>-</sup> T cells expanded exponentially at the portal of entry and distal sites in the LTs, the predominant expansion was in the HLA DR<sup>-</sup> and Ki67<sup>-</sup> T cell population (Fig. 1, panels HLA-DR and Ki67, and Tables 3 and 4). The major difference between the populations that were HLA-DR<sup>+</sup> and Ki67<sup>+</sup> or HLA-DR<sup>-</sup> and Ki67<sup>-</sup> was in the levels of viral gene expression. The mean number of silver grains determined by quantitative image analysis (QIA) (15, 21), which is proportional to the intracellular concentration of SIV RNA, was about four to seven times higher in the activated and proliferating HLA-DR<sup>+</sup> and Ki67<sup>+</sup> population (Tables 3 and 4). Despite the different levels of vRNA the SIV major core protein (Fig. 1, panel SIVp27) was detectable in both populations as further evidence of productive infection, even at low levels of vRNA.

The unexpected observation that SIV could replicate, albeit at low levels, in HLA-DR<sup>-</sup> and Ki67<sup>-</sup> T cells led us to seek evidence of a similar population in HIV-1 infection. We subsequently found and present evidence that, in HIV-1 infection from the earliest stages forward, most of the vRNA<sup>+</sup> cells are T cells; HIV-1 replicates in these cells whether or not they are demonstrably activated and proliferating; and the infected cells that are not proliferating have lower levels of viral gene expression and are longer lived.

We analyzed lymph node (LN) biopsies obtained from four individuals 2 to 15 days (mean 8 days) from the onset of symptoms of the acute retroviral syndrome, which occurs

REPORTS

**Table 5.** HIV-1 RNA in HLA-DR<sup>+</sup> or HLA-DR<sup>-</sup> and Ki67<sup>+</sup> or Ki67<sup>-</sup> T cells at early and late stages of infection and post-HAART LNs and tonsil biopsies were obtained from HIV-1-infected individuals in the acute, early and late stages of infection and post-HAART (22, 23, 25). With the specific activity and complexity of the HIV probes for autoradiographic exposures of 24 hours, infected cells with  $\geq 10$  copies of HIV-1 RNA were detected. The frequency of T cells with HIV-1 RNA was determined by counting

vRNA<sup>+</sup> cells in sections whose weight was calculated from the area, thickness, and density (16). This frequency  $\times$  percent CD3<sup>+</sup> cells gives the T cell frequency. Reduction after HAART was calculated from changes from baseline Ki67<sup>+</sup> or Ki67<sup>-</sup> population size in late-stage patients 2 days after initiating HAART. The percentage of CD3<sup>+</sup> T cells that were HLA-DR<sup>±</sup> or Ki67<sup>±</sup> and grain counts in these populations were determined as described (16).

State of infection	Number of patients	Percent vRNA <sup>+</sup> cells			Frequency of vRNA <sup>+</sup> T cells per gram of LT	Viral RNA levels (grain counts per cell)			
		CD3 <sup>+</sup>	HLA-DR <sup>+</sup>	Ki67 <sup>+</sup>		HLA-DR <sup>+</sup>	HLA-DR <sup>-</sup>	Ki67 <sup>+</sup>	Ki67 <sup>-</sup>
Acute	4	93	54	46	$1.1 \times 10^6$	654 $\pm$ 498	141 $\pm$ 81	752 $\pm$ 544	144 $\pm$ 84
Early	5	85	59	43	$1.9 \times 10^5$	610 $\pm$ 436	147 $\pm$ 69	722 $\pm$ 480	152 $\pm$ 75
Late	10	88	85	76	$2.9 \times 10^5$	NT	NT	538 $\pm$ 410	165 $\pm$ 105
Day 2 post-HAART	8	83	NT	36	$6.8 \times 10^4$	NT	NT	398 $\pm$ 312	150 $\pm$ 91

after an average incubation period of 12 days (22); five LN biopsies from individuals  $\geq 63$  days to 242 days postseroconversion; and 10 tonsillar biopsies from a previously described cohort (23) of individuals in the late stages of HIV-1 infection ( $< 200$  CD4<sup>+</sup> T cells per cubic millimeter of peripheral blood) (Table 5). In the acute and early stages of infection about 90% of the vRNA<sup>+</sup> cells are CD3<sup>+</sup> T cells. This was also the case in the late stages of HIV-1 infection and 2 days after HAART. In the acute and early stages of HIV-1 infection, like in SIV infection, about half the vRNA<sup>+</sup> cells were HLA-DR<sup>-</sup> and Ki67<sup>-</sup>, with a mean concentration of intracellular vRNA about two to five times lower than the activated population (Table 5). By the late stages of infection  $> 75\%$  of the vRNA<sup>+</sup> cells were HLA-DR<sup>+</sup> and Ki67<sup>+</sup>. The high percentage of infection of activated T cells in the late stages is consistent with the increased activation state characteristic of late infection (24). The increase in the percentage of T cells scored as activated vRNA<sup>+</sup> T cells over the course of infection also indicates that the combined IHC staining technique is sufficiently sensitive to monitor changes in the activation status of infected cells.

To assess the dynamics of infection in Ki67<sup>+</sup> or Ki67<sup>-</sup> populations, we determined changes in the relative population sizes post-HAART. Before treatment most of the vRNA<sup>+</sup> cells are Ki67<sup>+</sup> but after treatment most of the vRNA<sup>+</sup> T cells are Ki67<sup>-</sup> (Fig. 2 and Table 5) because of the disproportionate life spans of

infected T cells in the two populations. Two days after HAART, the Ki67<sup>+</sup> vRNA<sup>+</sup> population shrinks by a factor of 9, whereas there is only a 1.5-fold change in the Ki67<sup>-</sup> population. We had previously shown that the decay of vRNA<sup>+</sup> cells in tonsillar tissues in the cohort designated late-stage infection and day 2 post-HAART in Table 5 was multiphasic (23). The initial decline occurred in a population of cells with high concentrations of vRNA that produce the bulk of HIV-1 and turn over with a  $t_{1/2}$  of about 1 day. There was a slower decline in cells with smaller amounts of vRNA, and this chronically infected population persisted for 6 to 30 months after initiation of HAART (23, 25). The dramatic decrease in Ki67<sup>+</sup> vRNA<sup>+</sup> T cells immediately after HAART is consistent with the conclusion that the short-lived population of productively infected cells is composed of infected Ki67<sup>+</sup> T cells. We had found (23) that the longer lived population was not IHC stained by antibodies that identify Mφs and now conclude, based on the relatively stable population size after HAART, that this population consists mainly of Ki67<sup>-</sup>-infected T cells.

To further narrow down the position in the cell cycle of the infected T cells in the Ki67<sup>-</sup> population, we used antibodies to earlier markers of stages of the cycle (Table 6). Quiescent cells in G<sub>0</sub> that reenter the cell cycle resynthesize D cyclins and cyclin-dependent kinases (cdks) in early stages of the cycle (26). We found in the populations of vRNA<sup>+</sup> cells that there were also cyclin D3<sup>-</sup> and cdk6<sup>-</sup> cells as

well as double-labeled vRNA<sup>+</sup> cyclin D3<sup>+</sup> or cdk6<sup>+</sup> cells (Fig. 1, panels Cyclin D3 and cdk6, and Table 6). Moreover, there were vRNA<sup>+</sup> PCNA<sup>-</sup> cells (Table 6) under conditions in which cells in any stage of the cycle and even some cells in G<sub>0</sub> that recently exited the cycle will be labeled (27). We also characterized the activation state more fully and showed that there were vRNA<sup>+</sup> cells that either had or lacked early and other activation markers such as CD25, CD71, CD30, CD38, and CD134 (Table 6). Panel CD25 in Fig. 1 has examples of vRNA<sup>+</sup> cells that were CD25<sup>+</sup> or CD25<sup>-</sup>.

By all these criteria, the infected T cells would be categorized as resting T cells. However, in vivo, the infected cells must be in a different state than cultured T cells where, under most (20) conditions, resting T cells cannot be productively infected. One possible difference in vivo is that cytokines provide a semipermissive milieu in resting T cells for viral replication, just as G<sub>0</sub> cells can be transduced by HIV-1-based vectors when cultivated with cytokines (28). Another possibility is that the state of the infected T cells in vivo differs because survival of resting T cells in vivo depends on contact with major

**Table 6.** Early markers of T cell activation and proliferation in SIV or HIV RNA<sup>+</sup> cells. Percentage of viral RNA<sup>+</sup> cells that were not stained by the indicated antibodies was determined as described in the legend to Table 2A. NT, not tested.

Tissues	vRNA <sup>+</sup> cells not stained by antibodies to activation and cell cycle markers (%)							
	Cyclin D3 <sup>-</sup>	cdk6 <sup>-</sup>	PCNA <sup>-</sup>	CD25 <sup>-</sup>	CD71 <sup>-</sup>	CD30 <sup>-</sup>	CD38 <sup>-</sup>	CD134 <sup>-</sup>
SIV-infected axillary LN, day 12	79	97	76	65	86	93	NT	NT
HIV-infected LN, acute stage of infection	82	84	70	58	69	77	79	73

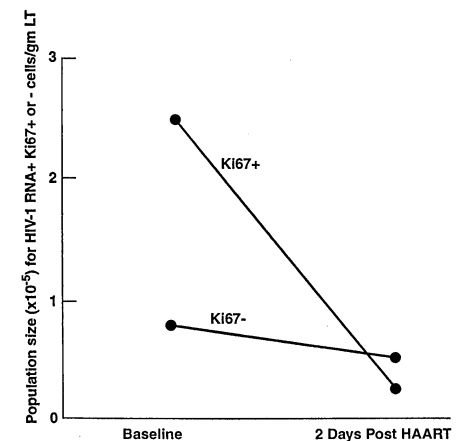


**Fig. 2.** Population size changes post-HAART in Ki67<sup>+</sup> or Ki67<sup>-</sup> vRNA<sup>+</sup> cells. Data from Table 5 are plotted at baseline and 2 days after initiation of HAART.

histocompatibility complex molecules (29). This low level of stimulation does not commit the cell to full activation and progression through the cell cycle but alters the state of the cell sufficiently to support viral replication at low levels. This altered state in vivo may be one explanation of why naive CD4<sup>+</sup> T cells in a constitutive resting state are infectable (30).

Infection of activated and resting populations of CD4<sup>+</sup> T cells could play critical and different roles in infection. The ability to infect and replicate in resting or perhaps minimally activated T cells could be particularly advantageous at transmission and in the early stages of infection. At these times, local propagation of infection must be sustained in an environment where it is less likely that the next host cell in the chain of transmission will be an activated T cell in the vicinity of the productively infected cell. The low level of viral gene expression could also provide a mechanism common to other lentivirus infections (31) for cells to elude host defenses and in this way favor establishment of a persistent infection. Persistent infection in the early stages of infection stands as an obstacle to prevention of infection by a vaccine. Infection of an activated T cell, on the other hand, is important because higher levels of virus production disseminate infection systemically and provide access to large numbers of target cells for continued replication. This creates conditions in LT in which activated cells are continuously generated to maintain the high levels of replication, sustain infection, and increase the chances of transmitting infection to another individual. The high levels of virus production and storage in LT cells also directly or indirectly compromise control of infection by the immune system. HAART can disrupt this vicious cycle, with documented benefits to the immune system (32), but leaves long-lived populations of latently (33) and chronically infected cells (23, 25) as obstacles to the long-term goal of eradication of virus and vaccine development.

References and Notes

1. R. A. Royce, A. Sena, W. Cates, M. S. Cohen, *N. Engl. J. Med.* **15**, 1072 (1997).
2. C. J. Miller, J. R. McGhee, M. B. Gardner, *Lab Invest.* **68**, 129 (1992).
3. J. O. Kahn and B. D. Walker, *N. Engl. J. Med.* **339**, 33 (1998).
4. C. J. Miller et al., *J. Med. Primatol.* **21**, 64 (1992).
5. A. B. van't Wout et al., *J. Clin. Invest.* **94**, 2060 (1994).
6. P. A. Marx et al., *Nature Med.* **2**, 1084 (1996).
7. A. I. Spira et al., *J. Exp. Med.* **183**, 215 (1996).
8. P. U. Cameron et al., *Science* **257**, 383 (1992).
9. M. Pope et al., *J. Exp. Med.* **182**, 2045 (1995).
10. M. Pope et al., *Cell* **78**, 389 (1994).
11. V. M. Hirsch et al., *Nature Med.* **4**, 1401 (1998).
12. C. J. Miller et al., *J. Virol.* **72**, 3248 (1998).
13. One primiparous and 13 multiparous adult rhesus monkeys (*M. mulatta*) were inoculated with uncloned SIV mac251 propagated in rhesus monkey peripheral blood mononuclear cells. Each monkey was anesthetized with ketamine and inoculated with 1 ml of tissue culture supernatant containing a 100% animal infectious dose of about 10<sup>5</sup> TCID<sub>50</sub> (median tissue culture infectious

dose) per milliliter of virus. The inoculum was instilled atraumatically into the vaginal vault. Another 1-ml dose was similarly introduced 4 hours later. To prevent loss of the inoculum, between and after inoculations the tranquilized animals were propped up in their cages so that the inoculum would drain toward the cervix. Four animals each 1, 3, and 7 days later, and 2 animals 12 days later, were euthanized. Tissues were collected and fixed in 10% neutral buffered formalin or Molecular Biology Fixative (Streck Laboratories, Omaha, NE). Animal maintenance and procedures were in accordance with the guidelines of the Committee on Animals for the Harvard Medical School and the *Guide for the Care and Use of Laboratory Animals* (National Research Council, National Academy Press, Washington, DC, 1996).

14. vRNA was detected by ISH with <sup>35</sup>S-labeled RNA probes as described (75). In brief, after fixed tissues were embedded in paraffin, 5-μm sections were cut, adhered to siliconized slides, and deparaffinized. Sections were then placed in 10 mM citric buffer (pH 6.2) and microwaved. After acetylation, sections were hybridized to SIV-specific RNA probes complementary to about 10% of the sequences at the 5' end of the SIV mac251 RNA genome labeled to specific activities of about 2 × 10<sup>9</sup> dpm/μg by incorporation of <sup>35</sup>S-labeled uridine triphosphate. HIV-1 was detected with a collection of RNA probes complementary to about 90% of the viral RNA radiolabeled to specific activities of about 6 × 10<sup>6</sup> dpm/μg. As controls, sections were also hybridized to virus-specific sense probes or tissues from mock-infected animals were hybridized to virus-specific antisense RNA probes. After hybridization, the slides were washed in 5× standard saline citrate (SSC), 10 mM dithiothreitol (DTT) at 42°C, 2× SSC, 10 mM DTT, 50% formamide at 60°C, and a 2× RWS buffer [0.1 M tris-HCl (pH 7.5), 0.4 M NaCl, 50 mM EDTA] before digestion at 37°C with ribonuclease A (25 μg/ml) and T<sub>1</sub> (25 units/ml) in 1× RWS. After washing in RWS, 2× SSC, and 0.1× SSC, sections were dehydrated in graded ethanol solutions containing 0.3 M ammonium acetate and then dried and coated with Kodak NTB-2 emulsion exposed at 4°C, developed, and stained.
15. A. T. Haase et al., *Science* **274**, 985 (1996).
16. SIV RNA<sup>+</sup> cells were detected by ISH with <sup>35</sup>S-labeled SIV-specific antisense RNA probe after autoradiographic exposures of 16.5 hours or 7 days. Nonspecific background was determined in two ways with equivalent results. Silver grains were counted over 100 cells in tissue sections from mock-inoculated uninfected monkeys after hybridization to the SIV antisense probe or over cells from the tissues of infected monkeys after hybridization to sense SIV-specific probe. In both cases the average background was 2.7 grains per cell for the 16.5-hour exposure. The Poisson probability that x number of grains differs from a background average of m is  $P = (m^x \times e^{-m})/x!$ . For a cell with ≥8 grains over background, the probability that the cell is infected is >0.99. By means of a previously validated (75) back-calculation of copy number (from grain counts, specific activity of probe, exposure time, and efficiency of image formation), we determined that 8 grains corresponds to about 15 copies of vRNA per cell. Cells that met this criterion were scored positive for vRNA. The relative frequency of vRNA<sup>+</sup> cells was normalized to an area of 1660 mm<sup>2</sup>, the area of 20 sections of endocervix that had to be screened 3 days postinoculation to detect vRNA<sup>+</sup> cells (that met the criterion described above for infection).
17. Cell type and activation status of viral RNA<sup>+</sup> cells was assessed by combined IHC staining and ISH as described (78). After ISH, washing, and digestion with ribonucleases, cells in the sections were stained by IHC with antibodies that stain T lymphocytes (antibody to CD3; rabbit polyclonal antibody to human; Dako, Carpinteria, CA), CD4<sup>+</sup> T cells (anti-CD4; NCL-CD4-IF6; Novocastra Laboratories, Newcastle, UK), Mφs (anti-CD68; KP1; Dako, Carpinteria, CA), and DCs (anti-S100; rabbit polyclonal antibody to cow; Dako, Carpinteria, CA). To assess T cell activation and cell cycle position in vRNA<sup>+</sup> cells, ISH to detect vRNA was combined with IHC staining antibodies that stain activated cells (HLA-DR, CD25, CD71, CD30, CD38, and CD134) and proliferating cells (Ki67, cyclin D3, cdk6, PCNA). We used dilutions of antibodies that had been determined to give optimal specific staining [for example, a 1:150 dilution of anti-HLA-DR clone Tal 1B5 from Dako, Carpinteria; CD25,

- 1:60 dilution, NeoMarker, Union City, CA; CD71, CD30, CD38, and CD134, 1:50 dilution, PharMingen, San Diego, CA; Ki67 monoclonal antibody (mAb), 1:100; cyclin D3 mAb, 1:10; PCNA mAb, 1:200, Novocastra Laboratories, Newcastle, UK; cdk6 mAb, 1:10, Santa Cruz Biotechnology, Santa Cruz, CA]. As a negative control, sections were reacted with a comparable concentration of the same isotype IgG1 κ (MoPc-31c; Sigma, St. Louis, MO). Sections were washed, nonspecific reactions were blocked with nonfat milk in phosphate-buffered saline (PBS), and the sections were reacted with primary antibody and then peroxidase-conjugated secondary antibody. Sections were IHC stained with H<sub>2</sub>O<sub>2</sub> and diaminobenzidine according to the manufacturer's protocol (ABC Elite kit, Vector 2 Labs, Burlingame, CA). After washing in PBS and 0.1× PBS, sections were dehydrated in a series of graded ethanol that contained 0.3 ammonium acetate and coated with nuclear track emulsion. After development, the slides were briefly counterstained in hematoxylin.
18. M. Brahic and A. T. Haase, *Curr. Topics Micro. Immun.* **143**, 9 (1989).
19. R. S. Veazey et al., *Science* **280**, 427 (1998); C. Stahl-Hennig et al., *Science* **285**, 1261 (1999).
20. J. A. Zack et al., *Cell* **61**, 213 (1990); J. A. Zack, A. M. Haislip, P. Krogstad, I. S. Y. Chen, *J. Virol.* **66**, 1717 (1992); Y. D. Korin and J. A. Zack, *J. Virol.* **72**, 3161 (1998); C.-S. Chou, O. Ramilo, E. S. Vitetta, *Proc. Natl. Acad. Sci. USA* **1361** (1997); S. Tang, B. Patterson, J. A. Levy, *J. Virol.* **69**, 5659 (1995); C. A. Spina, J. C. Guatelli, D. D. Richman, *J. Virol.* **69**, 2977 (1995); M. I. Burkinsky, T. L. Stanwick, M. P. Dempsey, M. Stevenson, *Science* **254**, 423 (1991).
21. As described in (75), infected cells were identified in the sections and the silver grain count was determined by QIA of autoradiographs illuminated by epipolarized light. Video images were captured with a low-light cooled charge-coupled device camera (Optronics TEC-470) and image 1/1MetaMorph version 2 software (Universal Imaging, Westchester, PA). Silver grains were distinguished from background and measured with the "threshold" and "measure object" tool of the MetaMorph software. The frequency of cells with vRNA in a defined area (in square millimeters) was determined with the calibration tool.
22. T. W. Schacker et al., *Ann. Int. Med.* **28**, 613 (1998).
23. W. Cavert et al., *Science* **276**, 960 (1997).
24. J. M. Orendi et al., *J. Infect. Dis.* **178**, 1279 (1998).
25. J. K. Wong et al., *Proc. Natl. Acad. Sci. U.S.A.* **94**, 12574 (1997).
26. C. J. Sherr, *Cell* **79**, 551 (1994).
27. R. Bravo and H. Macdonald-Brav, *J. Cell Biol.* **105**, 1549 (1987). PCNA is undetectable in quiescent cells in non-proliferating tissues but is detectable in cultured cells fixed with aldehydes for 24 to 48 hours after the cells have been growth arrested by serum starvation.
28. R. E. Sutton, H. T. M. Wu, R. Rigg, E. Bohnlein, P. O. Brown, *J. Virol.* **72**, 5781 (1998); R. E. Sutton, M. J. Reitsma, N. Uchida, P. O. Brown, *J. Virol.* **73**, 3649 (1999); D. Uhtmaz, S. Marmon, R. Sutton, V. N. Kewalramani, D. R. Littman, *J. Exp. Med.* **89**, 1735 (1999).
29. A. A. Freitas and B. Rocha, *Science* **277**, 1950 (1997); C. Benoist and D. Mathis, *Science* **276**, 2000 (1997); M. A. Markiewicz et al., *Proc. Natl. Acad. Sci. U.S.A.* **95**, 3065 (1998); C. Tanchot, F. A. Lemonnier, B. Perarnau, A. A. Freitas, B. Rocha, *Science* **276**, 2057 (1997).
30. M. A. Ostrowski et al., *J. Virol.* **73**, 6430 (1999).
31. A. T. Haase, *Nature* **332**, 130 (1986).
32. B. Autran et al., *Science* **277**, 112 (1997); G. Gorochov et al., *Nature Med.* **4**, 215 (1998); K. V. Komanduri et al., *Nature Med.* **4**, 953 (1998); E. S. Withers-Ward et al., *Nature Med.* **3**, 1102 (1997); Z.-Q. Zhang et al., *Proc. Natl. Acad. Sci. U.S.A.* **95**, 1154 (1998); Z.-Q. Zhang et al., *Proc. Natl. Acad. Sci. U.S.A.* **96**, 5169 (1999).
33. J. K. Wong et al., *Science* **278**, 1291 (1997); T.-W. Chun et al., *Proc. Natl. Acad. Sci. U.S.A.* **94**, 13193 (1997); D. Finzi et al., *Science* **278**, 1295 (1997).
34. Supported by the Great Lakes Regional Center for AIDS Research; NIH grants AI 28246, AI 38565, and RR 00168; and the German Ministry of Education and Research (BMBF 01 K-1-97146). We thank L. Shand, C. O'Neill, T. Leonard, and G. Sedgewick for preparation of the manuscript and figures and M. Dykhuizen and R. Evans for technical assistance.

10 June 1999; accepted 4 October 1999

## LINKED CITATIONS

- Page 1 of 5 -



You have printed the following article:

### **Sexual Transmission and Propagation of SIV and HIV in Resting and Activated CD4<sup>+</sup> T Cells**

Z.-Q. Zhang; T. Schuler; M. Zupancic; S. Wietgreffe; K. A. Staskus; K. A. Reimann; T. A. Reinhart; M. Rogan; W. Cavert; C. J. Miller; R. S. Veazey; D. Notermans; S. Little; S. A. Danner; D. D. Richman; D. Havlir; J. Wong; H. L. Jordan; T. W. Schacker; P. Racz; K. Tenner-Racz; N. L. Letvin; S. Wolinsky; A. T. Haase

*Science*, New Series, Vol. 286, No. 5443. (Nov. 12, 1999), pp. 1353-1357.

Stable URL:

<http://links.jstor.org/sici?sici=0036-8075%2819991112%293%3A286%3A5443%3C1353%3ASTAPOS%3E2.0.CO%3B2-E>

---

This article references the following linked citations:

## References and Notes

### <sup>8</sup> **Dendritic Cells Exposed to Human Immunodeficiency Virus Type-1 Transmit a Vigorous Cytopathic Infection to CD4<sup>+</sup> T Cells**

Paul U. Cameron; Peter S. Freudenthal; Jeanne M. Barker; Stuart Gezelter; Kayo Inaba; Ralph M. Steinman

*Science*, New Series, Vol. 257, No. 5068. (Jul. 17, 1992), pp. 383-387.

Stable URL:

<http://links.jstor.org/sici?sici=0036-8075%2819920717%293%3A257%3A5068%3C383%3ADCETHI%3E2.0.CO%3B2-J>

### <sup>15</sup> **Quantitative Image Analysis of HIV-1 Infection in Lymphoid Tissue**

Ashley T. Haase; Keith Henry; Mary Zupancic; Gerald Sedgewick; Russell A. Faust; Holly Melroe; Winston Cavert; Kristin Gebhard; Katherine Staskus; Zhi-Qiang Zhang; Peter J. Dailey; Henry H. Balfour Jr.; Alejo Erice; Alan S. Perelson

*Science*, New Series, Vol. 274, No. 5289. (Nov. 8, 1996), pp. 985-989.

Stable URL:

<http://links.jstor.org/sici?sici=0036-8075%2819961108%293%3A274%3A5289%3C985%3AQIAOHI%3E2.0.CO%3B2-O>

**NOTE:** The reference numbering from the original has been maintained in this citation list.

## LINKED CITATIONS

- Page 2 of 5 -



**<sup>19</sup> Gastrointestinal Tract as a Major Site of CD4<sup>+</sup>T Cell Depletion and Viral Replication in SIV Infection**

Ronald S. Veazey; MaryAnn DeMaria; Laura V. Chalifoux; Daniel E. Shvetz; Douglas R. Pauley; Heather L. Knight; Michael Rosenzweig; R. Paul Johnson; Ronald C. Desrosiers; Andrew A. Lackner

*Science*, New Series, Vol. 280, No. 5362. (Apr. 17, 1998), pp. 427-431.

Stable URL:

<http://links.jstor.org/sici?sici=0036-8075%2819980417%293%3A280%3A5362%3C427%3AGTAAMS%3E2.0.CO%3B2-G>

**<sup>19</sup> Rapid Infection of Oral Mucosal-Associated Lymphoid Tissue with Simian Immunodeficiency Virus**

Christiane Stahl-Hennig; Ralph M. Steinman; Klara Tenner-Racz; Melissa Pope; Nicole Stolte; Kerstin Mätz-Rensing; Gudrun Grobschupff; Birgit Raschdorff; Gerhard Hunsmann; Paul Racz  
*Science*, New Series, Vol. 285, No. 5431. (Aug. 20, 1999), pp. 1261-1265.

Stable URL:

<http://links.jstor.org/sici?sici=0036-8075%2819990820%293%3A285%3A5431%3C1261%3ARIOOML%3E2.0.CO%3B2-Q>

**<sup>20</sup> Highly Purified CD25<sup>+</sup> Resting T Cells Cannot be Infected de novo with HIV-1**

Chin-Sheng Chou; Octavio Ramilo; Ellen S. Vitetta

*Proceedings of the National Academy of Sciences of the United States of America*, Vol. 94, No. 4. (Feb. 18, 1997), pp. 1361-1365.

Stable URL:

<http://links.jstor.org/sici?sici=0027-8424%2819970218%2994%3A4%3C1361%3AHPCRTC%3E2.0.CO%3B2-K>

**<sup>23</sup> Kinetics of Response in Lymphoid Tissues to Antiretroviral Therapy of HIV-1 Infection**

Winston Cavert; Daan W. Notermans; Katherine Staskus; Stephen W. Wietgreffe; Mary Zupancic; Kristin Gebhard; Keith Henry; Zhi-Qiang Zhang; Roger Mills; Hugh McDade; Jaap Goudsmit; Sven A. Danner; Ashley T. Haase

*Science*, New Series, Vol. 276, No. 5314. (May 9, 1997), pp. 960-964.

Stable URL:

<http://links.jstor.org/sici?sici=0036-8075%2819970509%293%3A276%3A5314%3C960%3AKORILT%3E2.0.CO%3B2-2>

## LINKED CITATIONS

- Page 3 of 5 -



<sup>25</sup> **Reduction of HIV-1 in Blood and Lymph Nodes Following Potent Antiretroviral Therapy and the Virologic Correlates of Treatment Failure**

Joseph K. Wong; Huldrych F. Gunthard; Diane V. Havlir; Zhi-Qiang Zhang; Ashley T. Haase; Caroline C. Ignacio; Shirley Kwok; Emilio Emini; Douglas D. Richman

*Proceedings of the National Academy of Sciences of the United States of America*, Vol. 94, No. 23. (Nov. 11, 1997), pp. 12574-12579.

Stable URL:

<http://links.jstor.org/sici?sici=0027-8424%2819971111%2994%3A23%3C12574%3AROHIBA%3E2.0.CO%3B2-K>

<sup>29</sup> **Lymphocyte Survival: A Red Queen Hypothesis**

Antonio A. Freitas; Benedita Rocha

*Science*, New Series, Vol. 277, No. 5334. (Sep. 26, 1997), p. 1950.

Stable URL:

<http://links.jstor.org/sici?sici=0036-8075%2819970926%293%3A277%3A5334%3C1950%3ALSARQH%3E2.0.CO%3B2-2>

<sup>29</sup> **Selection for Survival?**

Christophe Benoist; Diane Mathis

*Science*, New Series, Vol. 276, No. 5321. (Jun. 27, 1997), pp. 2000-2001.

Stable URL:

<http://links.jstor.org/sici?sici=0036-8075%2819970627%293%3A276%3A5321%3C2000%3ASFSS%3E2.0.CO%3B2-D>

<sup>29</sup> **Long-Term T Cell Memory Requires the Surface Expression of Self-Peptide / Major Histocompatibility Complex Molecules**

Mary A. Markiewicz; Cristina Giraó; Joseph T. Opferman; Jiling Sun; Qinghui Hu; Alexander A. Agulnik; Colin E. Bishop; Craig B. Thompson; Philip G. Ashton-Rickardt

*Proceedings of the National Academy of Sciences of the United States of America*, Vol. 95, No. 6. (Mar. 17, 1998), pp. 3065-3070.

Stable URL:

<http://links.jstor.org/sici?sici=0027-8424%2819980317%2995%3A6%3C3065%3ALTCMRT%3E2.0.CO%3B2-R>

<sup>29</sup> **Differential Requirements for Survival and Proliferation of CD8 Naïve or Memory T Cells**

Corinne Tanchot; François A. Lemonnier; Beatrice Pérarnau; Antonio A. Freitas; Benedita Rocha

*Science*, New Series, Vol. 276, No. 5321. (Jun. 27, 1997), pp. 2057-2062.

Stable URL:

<http://links.jstor.org/sici?sici=0036-8075%2819970627%293%3A276%3A5321%3C2057%3ADRESAP%3E2.0.CO%3B2-9>

## LINKED CITATIONS

- Page 4 of 5 -



<sup>32</sup> **Positive Effects of Combined Antiretroviral Therapy on CD4<sup>+</sup> T Cell Homeostasis and Function in Advanced HIV Disease**

B. Autran; G. Carcelain; T. S. Li; C. Blanc; D. Mathez; R. Tubiana; C. Katlama; P. Debré; J. Leibowitch

*Science*, New Series, Vol. 277, No. 5322. (Jul. 4, 1997), pp. 112-116.

Stable URL:

<http://links.jstor.org/sici?sici=0036-8075%2819970704%293%3A277%3A5322%3C112%3APEOCAT%3E2.0.CO%3B2-B>

<sup>32</sup> **Kinetics of CD4<sup>+</sup> T Cell Repopulation of Lymphoid Tissues after Treatment of HIV-1 Infection**

Zhi-Qiang Zhang; Daan W. Notermans; Gerald Sedgewick; Winston Cavert; Stephen Wietgreffe; Mary Zupancic; Kristin Gebhard; Keith Henry; Lawrence Boies; Zongming Chen; Marc Jenkins; Roger Mills; Hugh McDade; Carolyn Goodwin; Caspar M. Schuwirth; Sven A. Danner; Ashley T. Haase

*Proceedings of the National Academy of Sciences of the United States of America*, Vol. 95, No. 3. (Feb. 3, 1998), pp. 1154-1159.

Stable URL:

<http://links.jstor.org/sici?sici=0027-8424%2819980203%2995%3A3%3C1154%3AKOCTCR%3E2.0.CO%3B2-W>

<sup>32</sup> **Reversibility of the Pathological Changes in the Follicular Dendritic Cell Network with Treatment of HIV-1 Infection**

Zhi-Qiang Zhang; Troy Schuler; Winston Cavert; Daan W. Notermans; Kristin Gebhard; Keith Henry; Diane V. Havlir; Huldrych F. Gunthard; Joseph K. Wong; Susan Little; Mark B. Feinberg; Michael A. Polis; Lewis K. Schragar; Timothy W. Schacker; Douglas D. Richman; Lawrence Corey; Sven A. Danner; Ashley T. Haase

*Proceedings of the National Academy of Sciences of the United States of America*, Vol. 96, No. 9. (Apr. 27, 1999), pp. 5169-5172.

Stable URL:

<http://links.jstor.org/sici?sici=0027-8424%2819990427%2996%3A9%3C5169%3AROTPCI%3E2.0.CO%3B2-U>

<sup>33</sup> **Recovery of Replication-Competent HIV Despite Prolonged Suppression of Plasma Viremia**

Joseph K. Wong; Marjan Hezareh; Huldrych F. Gunthard; Diane V. Havlir; Caroline C. Ignacio; Celsa A. Spina; Douglas D. Richman

*Science*, New Series, Vol. 278, No. 5341. (Nov. 14, 1997), pp. 1291-1295.

Stable URL:

<http://links.jstor.org/sici?sici=0036-8075%2819971114%293%3A278%3A5341%3C1291%3ARORHDP%3E2.0.CO%3B2-L>

## LINKED CITATIONS

- Page 5 of 5 -



<sup>33</sup> **Presence of an Inducible HIV-1 Latent Reservoir during Highly Active Antiretroviral Therapy**

Tae-Wook Chun; Lieven Stuyver; Stephanie B. Mizell; Linda A. Ehler; Jo Ann M. Mican; Michael Baseler; Alun L. Lloyd; Martin A. Nowak; Anthony S. Fauci

*Proceedings of the National Academy of Sciences of the United States of America*, Vol. 94, No. 24. (Nov. 25, 1997), pp. 13193-13197.

Stable URL:

<http://links.jstor.org/sici?sici=0027-8424%2819971125%2994%3A24%3C13193%3APOAIHL%3E2.0.CO%3B2-F>

<sup>33</sup> **Identification of a Reservoir for HIV-1 in Patients on Highly Active Antiretroviral Therapy**

Diana Finzi; Monika Hermankova; Theodore Pierson; Lucy M. Carruth; Christopher Buck; Richard E. Chaisson; Thomas C. Quinn; Karen Chadwick; Joseph Margolick; Ronald Brookmeyer; Joel Gallant; Martin Markowitz; David D. Ho; Douglas D. Richman; Robert F. Siliciano

*Science*, New Series, Vol. 278, No. 5341. (Nov. 14, 1997), pp. 1295-1300.

Stable URL:

<http://links.jstor.org/sici?sici=0036-8075%2819971114%293%3A278%3A5341%3C1295%3AIOARFH%3E2.0.CO%3B2-Z>